

# Wigner Distributions For Gluons

Jai More<sup>a</sup>, Asmita Mukherjee<sup>a</sup> and Sreeraj Nair<sup>b</sup>

<sup>a</sup> *Department of Physics,*

*Indian Institute of Technology Bombay,*

*Powai, Mumbai 400076, India.*

<sup>b</sup> *Department of Physics,*

*Indian Institute of Science Education and Research Bhopal*

*Bhopal Bypass Road, Bhauri, Bhopal 462066 India*

(Dated: December 14, 2024)

## Abstract

We investigate the gluon Wigner distributions for unpolarized, longitudinally polarized and transversely polarized target state. Instead of a nucleon, we take the target state to be a quark dressed with a gluon at one loop and investigate the gluon Wigner distributions at leading twist. Better numerical convergence is obtained compared to an earlier study, that removes the regulator dependence of the results. We present a first calculation of the Wigner distribution for the transversely polarized target and linearly polarized gluon. We study the spin densities in momentum and impact parameter space. We also investigate a relation between gluon orbital angular momentum and helicity at small- $x$ .

## I. INTRODUCTION

Nucleon spin puzzle has been a provoking issue since a couple of decades and the goal is to study, explore and understand the three dimensional picture of hadrons in terms of quarks and gluons. The generalized parton correlation functions (GPCFs)[1] provide a framework to study the composite structure of hadrons. GPCFs are fully unintegrated off diagonal quark-quark correlator which are functions of 4-momentum of quark and 4-momentum  $\Delta$ , which is transferred by the hadrons and contains a wealth of information of the nucleon. The GPCFs are also related to quantum mechanical analogue of classical phase space distribution called as Wigner distributions [2–4]. On integrating the GPCFs over the light front energy ( $k^-$ ) one obtains generalized transverse-momentum-dependent distributions (GTMDs). GTMDs and the Wigner distributions are Fourier transforms of each other [1, 5]. The matrix element of Wigner distributions are six dimensional and are functions of three position and three momentum variables [3, 4]. It is convenient to use a five-dimensional Wigner distribution as a function of two transverse positions and three momentum coordinates in light-front formalism [6]. These are often considered as mother distributions of the transverse-momentum dependent distribution (TMDs)[7–9] and generalized parton distributions (GPDs) [10–16]. GPDs are obtained by integrating Wigner distribution over transverse momentum  $\mathbf{k}_\perp$  while TMDs are obtained by integrating the Wigner distributions over the transverse position  $\mathbf{b}_\perp$ .

Wigner distributions are not always positive definite. So far the Wigner distributions of quarks and gluon have only been studied through model calculations, for example in constituent quark model and chiral quark soliton model [6], spectator model [17] and holographic model [18, 19]. Wigner distributions of nucleons in a nucleus were studied in [20]. Very recently the possibility to access the quark GTMDs in an exclusive double Drell-Yan process has been investigated in [21]. Most of the models have no gluonic degrees of freedom, and so gluon GTMDs and gluon Wigner distributions cannot be investigated in such models. Although interest in quark GTMDs are rather recent, gluon GTMDs and unintegrated gluon correlators have been introduced and discussed in the context of small  $x$  physics for diffractive vector meson production [22] and for Higgs production at Tevatron and LHC [23] quite some time back. The details of operator definitions, as well as parametrizations of gluon GTMDs, are given in [24]. There is also a growing interest to understand how to

probe the gluon GTMDs experimentally that are related to the gluon Wigner distributions by a Fourier transform. In [25] the authors proposed to study small  $x$  gluon GTMDs in diffractive dijet production, and also in [26] for correlated hard diffractive dijet production in deep inelastic scattering. Exclusive dijets in deep inelastic scattering within the formalism of color glass condensate was first studied in [27]. Elliptic gluon GTMDs were studied in [28]. In [29] the authors proposed to probe the gluon GTMDs and Wigner distributions in DVCS at small  $x$ . In [30] gluon Wigner and Husimi distributions were investigated. Husimi distributions contain a Gaussian factor in the integrand that makes them positive definite, unlike Wigner distributions that are not positive definite. The disadvantage is that upon integration, the Husimi distributions do not reduce to known TMDs [31] suggested to probe the gluon Wigner distributions in ultra-peripheral  $pA$  collision.

Compared to the quark GTMDs, gluon GTMDs and Wigner distributions have more complex process dependence due to the presence of two gauge links in the gluon correlator required by color gauge invariance [32–34], the simplest combinations are  $++$  (Weizsacker-Williams or WW-type) and  $+ -$  (dipole type). Recent interest in quark and gluon Wigner distributions and GTMDs is related to the fact that these can provide important information about the so far unknown quark and gluon orbital angular momentum (OAM) in the nucleon [35–38]. It was shown in [25] that both the WW type and dipole type gluon GTMDs give the same gluon OAM distribution. In models of the nucleon without gluonic degrees of freedom, one cannot study the gluon Wigner distributions/GTMDs. The possibility to probe the gluon Wigner distribution and gluon orbital angular momentum at the future electron-ion collider was studied in [39]. In [40, 41] we investigated the quark and gluon Wigner distributions and OAM for a simple composite spin- $\frac{1}{2}$  target state, namely for a quark dressed with a gluon at one loop in QCD. This may be considered as a field theory inspired perturbative model having a gluonic degree of freedom. The quark has non-zero mass and both quark and gluon have non-zero transverse momenta. Wigner distributions were expressed in terms of overlaps of light-front wave functions (LFWFs), which were calculated analytically in light-front Hamiltonian perturbation theory. In [41] we calculated the quark Wigner distributions for the unpolarized and longitudinally polarized target. The results were found to depend on a regulator on the momentum transfer by the target in the transverse direction. The convergence was improved, and the regulator dependence was removed in the quark Wigner distributions in [42] and transverse polarization was included.

Here we continue our study and calculate the gluon Wigner distributions, using improved numerical convergence, and remove the regulator dependence present in the earlier work [40]. We also include transverse and linear polarization in the study of gluon Wigner distributions at leading twist.

The manuscript is organized in the following manner. In Sec. II, we begin with the field theory definition of the gluon Wigner distribution. We give the analytical expressions for gluon Wigner distribution at leading twist in the dressed quark model. In Sec. III, we explain the numerical strategy used for studying the Wigner distribution followed by the discussion of our numerical results. In Sec. IV We discuss spin density in transverse momentum and transverse position space. We investigate a small- $x$  relation between the gluon orbital angular momentum and helicity in our model in Sec. V. Conclusions are given in Sec. VI.

## II. GLUON WIGNER DISTRIBUTIONS IN DRESSED QUARK MODEL

The Wigner distribution of gluon can be defined as [1, 6]

$$\begin{aligned}
xW_{\sigma,\sigma'}(x, \mathbf{k}_\perp, \mathbf{b}_\perp) &= \int \frac{d^2\Delta_\perp}{(2\pi)^2} e^{-i\Delta_\perp \cdot \mathbf{b}_\perp} \int \frac{dz^- d^2\mathbf{z}_\perp}{2(2\pi)^3 p^+} e^{ik \cdot z} \\
&\times \left\langle p^+, -\frac{\Delta_\perp}{2}, \sigma' \left| \Gamma^{ij} F^{+i} \left( -\frac{z}{2} \right) F^{+j} \left( \frac{z}{2} \right) \right| p^+, \frac{\Delta_\perp}{2}, \sigma \right\rangle_{z^+=0}
\end{aligned} \quad (1)$$

where  $\Delta_\perp$  and  $\mathbf{b}_\perp$  is the transverse momentum transfer from the target state and impact parameter space variable respectively.  $\mathbf{b}_\perp$  is conjugate to  $\Delta_\perp$ , the gluon field strength tensor is given by

$$F_a^{+i} = \partial^+ A_a^i - \partial^i A_a^+ + g f_{abc} A_b^+ A_c^i \quad (2)$$

The operator structure for gluon at twist two are [24] (i)  $\Gamma^{ij} = \delta_\perp^{ij}$ , (ii)  $\Gamma^{ij} = -i\epsilon_\perp^{ij}$  (iii)  $\Gamma^{ij} = \Gamma^{RR}$  and (iv)  $\Gamma^{ij} = \Gamma^{LL}$ , where  $L(R)$  are left(right) polarization of the gluon (to be defined later). We have suppressed the color indices. The above correlator needs two gauge links for color gauge invariance. We choose light-cone gauge and take the gauge link to be unity, that is we will not be calculating the effect of the transverse link at light-cone infinity. In the previous work [42], we discussed the quark Wigner distribution for the dressed quark model. The dressed quark state with momentum ' $p$ ' and helicity ' $s$ ' can be written in terms

of light-front wave functions (LFWFs) as the expansion of the state in Fock space:

$$\begin{aligned} |p^+, \mathbf{p}_\perp, s\rangle &= \Phi^s(p) b_s^\dagger(p) |0\rangle + \sum_{s_1 s_2} \int \frac{dp_1^+ d^2 \mathbf{p}_1^\perp}{\sqrt{16\pi^3 p_1^+}} \int \frac{dp_2^+ d^2 \mathbf{p}_2^\perp}{\sqrt{16\pi^3 p_2^+}} \sqrt{16\pi^3 p^+} \\ &\times \delta^3(p - p_1 - p_2) \Phi_{s_1 s_2}^s(p; p_1, p_2) b_{s_1}^\dagger(p_1) a_{s_2}^\dagger(p_2) |0\rangle \end{aligned} \quad (3)$$

where  $\Phi_{s_1 s_2}^s(p; p_1, p_2)$  is the two-particle LFWF.  $\Phi^s(p)$  gives the wave function normalization [43].  $\Phi_{s_1 s_2}^s(p; p_1, p_2)$  gives the probability amplitude to find a bare quark (gluon) with momentum  $p_1(p_2)$  and helicity  $s_1(s_2)$  inside the dressed quark. Using the Jacobi momenta

$$k_i^+ = x_i P^+ \quad \text{and} \quad \mathbf{k}_i^\perp = \mathbf{q}_i^\perp + x_i \mathbf{P}^\perp \quad (4)$$

so that

$$\sum_i x_i = 1, \quad \sum_i \mathbf{q}_i^\perp = 0 \quad (5)$$

the two-particle LFWF can be written in terms of the boost-invariant variables as

$$\sqrt{P^+} \Phi(p; p_1, p_2) = \Psi(x_i, \mathbf{q}_i^\perp) \quad (6)$$

$\mathbf{k}_\perp$  is the average transverse momentum of the gluon and  $x$  is the momentum fraction of the gluon. This LFWF can be calculated analytically using light-front Hamiltonian perturbation theory [43]. The gluon-gluon correlators in terms of overlap of two-particle LFWFs are given by

i) For  $\Gamma^{ij} = \delta_\perp^{ij}$

$$\mathcal{W}_{\sigma\sigma'}^1(x, \mathbf{k}_\perp, \Delta_\perp) = - \sum_{\sigma_1, \lambda_1, \lambda_2} \left[ \Psi_{\sigma_1 \lambda_1}^{*\sigma'}(\hat{x}, \hat{\mathbf{q}}'_\perp) \Psi_{\sigma_1 \lambda_2}^\sigma(\hat{x}, \hat{\mathbf{q}}_\perp) \left( \epsilon_{\lambda_2}^1 \epsilon_{\lambda_1}^{*1} + \epsilon_{\lambda_2}^2 \epsilon_{\lambda_1}^{*2} \right) \right] \quad (7)$$

ii) For  $\Gamma^{ij} = -i\epsilon_\perp^{ij}$

$$\mathcal{W}_{\sigma\sigma'}^2(x, \mathbf{k}_\perp, \Delta_\perp) = -i \sum_{\sigma_1, \lambda_1, \lambda_2} \left[ \Psi_{\sigma_1 \lambda_1}^{*\sigma'}(\hat{x}, \hat{\mathbf{q}}'_\perp) \Psi_{\sigma_1 \lambda_2}^\sigma(\hat{x}, \hat{\mathbf{q}}_\perp) \left( \epsilon_{\lambda_2}^1 \epsilon_{\lambda_1}^{*2} - \epsilon_{\lambda_2}^2 \epsilon_{\lambda_1}^{*1} \right) \right] \quad (8)$$

iii) For  $\Gamma^{RR}$

$$\mathcal{W}_{\sigma\sigma'}^3(x, \mathbf{k}_\perp, \Delta_\perp) = - \sum_{\sigma_1, \lambda_1, \lambda_2} \left[ \Psi_{\sigma_1 \lambda_1}^{*\sigma'}(\hat{x}, \hat{\mathbf{q}}'_\perp) \Psi_{\sigma_1 \lambda_2}^\sigma(\hat{x}, \hat{\mathbf{q}}_\perp) \epsilon_{\lambda_2}^R \epsilon_{\lambda_1}^{*R} \right] \quad (9)$$

iv) For  $\Gamma^{LL}$

$$\mathcal{W}_{\sigma\sigma'}^4(x, \mathbf{k}_\perp, \mathbf{\Delta}_\perp) = - \sum_{\sigma_1, \lambda_1, \lambda_2} \left[ \Psi_{\sigma_1 \lambda_1}^{*\sigma'}(\hat{x}, \hat{\mathbf{q}}'_\perp) \Psi_{\sigma_1 \lambda_2}^\sigma(\hat{x}, \hat{\mathbf{q}}_\perp) \epsilon_{\lambda_2}^L \epsilon_{\lambda_1}^{*L} \right] \quad (10)$$

where  $\hat{x} = (1 - x)$ ,  $\hat{\mathbf{q}}_\perp = -\mathbf{q}_\perp$ ,  $\mathbf{q}_\perp = \mathbf{k}_\perp + \frac{\mathbf{\Delta}_\perp}{2}(1 - x)$ ,  $\mathbf{q}'_\perp = \mathbf{k}_\perp - \frac{\mathbf{\Delta}_\perp}{2}(1 - x)$ . We choose the gluon right (left) polarization as  $\epsilon_\lambda^{R(L)} = \epsilon_\lambda^1 \pm i\epsilon_\lambda^2$ . Wigner distribution is obtained by taking the Fourier transform of Eqs. (7)-(10) and is given by

$$xW^\alpha(x, \mathbf{k}_\perp, \mathbf{b}_\perp, \hat{\mathbf{e}}) = \int \frac{d^2 \mathbf{\Delta}_\perp}{2(2\pi)^2} e^{-i\mathbf{\Delta}_\perp \cdot \mathbf{b}_\perp} \mathcal{W}_{\sigma\sigma}^\alpha(x, \mathbf{k}_\perp, \mathbf{\Delta}_\perp) \quad (11)$$

with  $\alpha = 1, 2, 3, 4$ . Thus, for different polarization of gluon viz (U) unpolarized, (L) longitudinally polarized and two ( $\mathcal{T}$ ) linearly polarized, one obtains 16 gluon Wigner distributions at leading twist. In the above expression, the polarization of the target state is denoted by  $\hat{\mathbf{e}}$ .  $T$  denotes the transverse polarization of the target. We denote the gluon Wigner distribution as  $W_{\lambda\lambda'}$ , where  $\lambda$  and  $\lambda'$  are the polarization of target state and gluon respectively. We categorize 16 Wigner distributions for different polarization combinations at leading twist.

### A. Unpolarized target and different gluon polarization

The unpolarized Wigner distribution

$$W_{UU}(x, \mathbf{k}_\perp, \mathbf{b}_\perp) = \frac{1}{2} \left[ W^1(x, \mathbf{k}_\perp, \mathbf{b}_\perp, \hat{\mathbf{e}}_z) + W^1(x, \mathbf{k}_\perp, \mathbf{b}_\perp, -\hat{\mathbf{e}}_z) \right] \quad (12)$$

The unpolarized-longitudinally polarized Wigner distribution

$$W_{UL}(x, \mathbf{k}_\perp, \mathbf{b}_\perp) = \frac{1}{2} \left[ W^2(x, \mathbf{k}_\perp, \mathbf{b}_\perp, \hat{\mathbf{e}}_z) + W^2(x, \mathbf{k}_\perp, \mathbf{b}_\perp, -\hat{\mathbf{e}}_z) \right] \quad (13)$$

The unpolarized-linearly polarized Wigner distribution

$$W_{U\mathcal{T}}^{(R)}(x, \mathbf{k}_\perp, \mathbf{b}_\perp) = \frac{1}{2} \left[ W^3(x, \mathbf{k}_\perp, \mathbf{b}_\perp, \hat{\mathbf{e}}_z) + W^3(x, \mathbf{k}_\perp, \mathbf{b}_\perp, -\hat{\mathbf{e}}_z) \right] \quad (14)$$

$$W_{U\mathcal{T}}^{(L)}(x, \mathbf{k}_\perp, \mathbf{b}_\perp) = \frac{1}{2} \left[ W^4(x, \mathbf{k}_\perp, \mathbf{b}_\perp, \hat{\mathbf{e}}_z) + W^4(x, \mathbf{k}_\perp, \mathbf{b}_\perp, -\hat{\mathbf{e}}_z) \right] \quad (15)$$

The superscript ' $L(R)$ ' represents left (right) polarization of gluon.

## B. Longitudinal polarized target and different gluon polarization

The longitudinal-unpolarized Wigner distribution

$$W_{LU}(x, \mathbf{k}_\perp, \mathbf{b}_\perp) = \frac{1}{2} \left[ W^1(x, \mathbf{k}_\perp, \mathbf{b}_\perp, \hat{e}_z) - W^1(x, \mathbf{k}_\perp, \mathbf{b}_\perp, -\hat{e}_z) \right] \quad (16)$$

The longitudinal Wigner distribution

$$W_{LL}(x, \mathbf{k}_\perp, \mathbf{b}_\perp) = \frac{1}{2} \left[ W^2(x, \mathbf{k}_\perp, \mathbf{b}_\perp, \hat{e}_z) - W^2(x, \mathbf{k}_\perp, \mathbf{b}_\perp, -\hat{e}_z) \right] \quad (17)$$

The longitudinal-linearly polarized Wigner distribution

$$W_{LT}^{(R)}(x, \mathbf{k}_\perp, \mathbf{b}_\perp) = \frac{1}{2} \left[ W^3(x, \mathbf{k}_\perp, \mathbf{b}_\perp, \hat{e}_z) - W^3(x, \mathbf{k}_\perp, \mathbf{b}_\perp, -\hat{e}_z) \right] \quad (18)$$

$$W_{LT}^{(L)}(x, \mathbf{k}_\perp, \mathbf{b}_\perp) = \frac{1}{2} \left[ W^4(x, \mathbf{k}_\perp, \mathbf{b}_\perp, \hat{e}_z) - W^4(x, \mathbf{k}_\perp, \mathbf{b}_\perp, -\hat{e}_z) \right] \quad (19)$$

## C. Transversely polarized target and different gluon polarization

The transversely polarized unpolarized Wigner distribution

$$W_{TU}^i(x, \mathbf{k}_\perp, \mathbf{b}_\perp) = \frac{1}{2} \left[ W^1(x, \mathbf{k}_\perp, \mathbf{b}_\perp, \hat{e}_i) - W^1(x, \mathbf{k}_\perp, \mathbf{b}_\perp, -\hat{e}_i) \right] \quad (20)$$

The transversely-longitudinally polarized Wigner distribution

$$W_{TL}^i(x, \mathbf{k}_\perp, \mathbf{b}_\perp) = \frac{1}{2} \left[ W^2(x, \mathbf{k}_\perp, \mathbf{b}_\perp, \hat{e}_i) - W^2(x, \mathbf{k}_\perp, \mathbf{b}_\perp, -\hat{e}_i) \right] \quad (21)$$

The transversely-linearly polarized Wigner distribution

$$W_{TT}^{i(R)}(x, \mathbf{k}_\perp, \mathbf{b}_\perp) = \frac{1}{2} \left[ W^3(x, \mathbf{k}_\perp, \mathbf{b}_\perp, \hat{e}_i) - W^3(x, \mathbf{k}_\perp, \mathbf{b}_\perp, -\hat{e}_i) \right] \quad (22)$$

$$W_{TT}^{i(L)}(x, \mathbf{k}_\perp, \mathbf{b}_\perp) = \frac{1}{2} \left[ W^4(x, \mathbf{k}_\perp, \mathbf{b}_\perp, \hat{e}_i) - W^4(x, \mathbf{k}_\perp, \mathbf{b}_\perp, -\hat{e}_i) \right] \quad (23)$$

where  $i$  denotes the transverse directions.  $\hat{e}_i$  correspond to the transverse polarization of the target state and these can be expressed as a linear combination of helicity states. We have chosen the transverse polarization to be in  $x$  direction.

Using the analytic expression of the two-particle LFWFs, we calculate the Wigner distributions. Expressions for the unpolarized and longitudinal polarization have been given earlier in [40]. For completeness, here we give them again and include the expressions for

transverse/linear polarizations also. The analytical expression for six linearly independent gluon Wigner distributions are given as:

$$W_{UU}(x, \mathbf{k}_\perp, \mathbf{b}_\perp) = N \int \frac{d^2 \Delta_\perp}{2(2\pi)^2} \frac{\cos(\Delta_\perp \cdot \mathbf{b}_\perp)}{D(\mathbf{q}_\perp)D(\mathbf{q}'_\perp)} \times \left[ -\frac{4m^2 x^4 + (x^2 - 2x + 2)(4\mathbf{k}_\perp^2 - \Delta_\perp^2(1-x)^2)}{(1-x)^2 x^3} \right] \quad (24)$$

$$W_{UL}(x, \mathbf{k}_\perp, \mathbf{b}_\perp) = N \int \frac{d^2 \Delta_\perp}{2(2\pi)^2} \frac{\sin(\Delta_\perp \cdot \mathbf{b}_\perp)}{D(\mathbf{q}_\perp)D(\mathbf{q}'_\perp)} \frac{4(x^2 - 2x + 2)(\Delta_y k_x - \Delta_x k_y)}{(1-x)x^3} \quad (25)$$

$$W_{LU}(x, \mathbf{k}_\perp, \mathbf{b}_\perp) = N \int \frac{d^2 \Delta_\perp}{2(2\pi)^2} \frac{\sin(\Delta_\perp \cdot \mathbf{b}_\perp)}{D(\mathbf{q}_\perp)D(\mathbf{q}'_\perp)} \frac{4(2-x)(\Delta_y k_x - \Delta_x k_y)}{(1-x)x^2} \quad (26)$$

$$W_{LL}(x, \mathbf{k}_\perp, \mathbf{b}_\perp) = N \int \frac{d^2 \Delta_\perp}{2(2\pi)^2} \frac{\cos(\Delta_\perp \cdot \mathbf{b}_\perp)}{D(\mathbf{q}_\perp)D(\mathbf{q}'_\perp)} \times \left[ -\frac{4m^2 x^3 + (2-x)(4\mathbf{k}_\perp^2 - \Delta_\perp^2(1-x)^2)}{(1-x)^2 x^2} \right] \quad (27)$$

$$W_{TU}^x(x, \mathbf{k}_\perp, \mathbf{b}_\perp) = N \int \frac{d^2 \Delta_\perp}{2(2\pi)^2} \frac{\sin(\Delta_\perp \cdot \mathbf{b}_\perp)}{D(\mathbf{q}_\perp)D(\mathbf{q}'_\perp)} \frac{4m\Delta_x}{x} \quad (28)$$

$$W_{TL}^x(x, \mathbf{k}_\perp, \mathbf{b}_\perp) = N \int \frac{d^2 \Delta_\perp}{2(2\pi)^2} \frac{\cos(\Delta_\perp \cdot \mathbf{b}_\perp)}{D(\mathbf{q}_\perp)D(\mathbf{q}'_\perp)} \frac{8mk_y}{x(1-x)} \quad (29)$$

where,  $N = \frac{g^2 C_F}{2(2\pi)^3}$ ,  $C_F$  is the color factor

$$D(\mathbf{q}_\perp) = \left[ m^2 - \frac{m^2 + (\mathbf{k}_\perp + \frac{\Delta_\perp(1-x)}{2})^2}{1-x} - \frac{(\mathbf{k}_\perp + \frac{\Delta_\perp(1-x)}{2})^2}{x} \right] \quad (30)$$

$$D(\mathbf{q}'_\perp) = \left[ m^2 - \frac{m^2 + (\mathbf{k}_\perp - \frac{\Delta_\perp(1-x)}{2})^2}{1-x} - \frac{(\mathbf{k}_\perp - \frac{\Delta_\perp(1-x)}{2})^2}{x} \right] \quad (31)$$

The remaining six gluon Wigner distributions can be expressed as linear combinations of

the above six distributions in this model as:

$$W_{UT}^{(R)}(x, \mathbf{k}_\perp, \mathbf{b}_\perp) = W_{UU}(x, \mathbf{k}_\perp, \mathbf{b}_\perp) - W_{UL}(x, \mathbf{k}_\perp, \mathbf{b}_\perp) \quad (32)$$

$$W_{UT}^{(L)}(x, \mathbf{k}_\perp, \mathbf{b}_\perp) = W_{UU}(x, \mathbf{k}_\perp, \mathbf{b}_\perp) + W_{UL}(x, \mathbf{k}_\perp, \mathbf{b}_\perp) \quad (33)$$

$$W_{LT}^{(R)}(x, \mathbf{k}_\perp, \mathbf{b}_\perp) = -W_{LL}(x, \mathbf{k}_\perp, \mathbf{b}_\perp) + W_{LU}(x, \mathbf{k}_\perp, \mathbf{b}_\perp) \quad (34)$$

$$W_{LT}^{(L)}(x, \mathbf{k}_\perp, \mathbf{b}_\perp) = W_{LL}(x, \mathbf{k}_\perp, \mathbf{b}_\perp) + W_{LU}(x, \mathbf{k}_\perp, \mathbf{b}_\perp) \quad (35)$$

$$W_{TT}^{(R)x}(x, \mathbf{k}_\perp, \mathbf{b}_\perp) = -W_{TL}^x(x, \mathbf{k}_\perp, \mathbf{b}_\perp) + W_{TU}^x(x, \mathbf{k}_\perp, \mathbf{b}_\perp) \quad (36)$$

$$W_{TT}^{(L)x}(x, \mathbf{k}_\perp, \mathbf{b}_\perp) = W_{TL}^x(x, \mathbf{k}_\perp, \mathbf{b}_\perp) + W_{TU}^x(x, \mathbf{k}_\perp, \mathbf{b}_\perp) \quad (37)$$

### III. NUMERICAL CALCULATIONS

The gluon Wigner distribution is a five-dimensional phase space distribution with two transverse components ( $\mathbf{k}_\perp, \mathbf{b}_\perp$ ) and a longitudinal momentum fraction ( $x$ ). In the following, we integrate out the longitudinal momentum fraction ( $x$ ) and study its behavior in the transverse phase space ( $\mathbf{k}_\perp, \mathbf{b}_\perp$ ). The Fourier transform over  $\Delta_\perp$  should go from  $-\infty$  to  $\infty$  in an ideal case, however, to perform numerical integration we follow Levin method [44–46] as we did to study quark Wigner distributions in our earlier work [42].

Figure. 1 shows the plot for the six linearly independent gluon Wigner distributions as a function of  $\Delta_{max}$ . Figure. 1 (a) shows the results when we apply Levin method whereas Fig. 1 (b) is generated using Monte Carlo method. Both plots are for the fixed value of  $b_x = 0.4 \text{ GeV}^{-1}, b_y = 0.5 \text{ GeV}^{-1}, k_x = 0.0 \text{ GeV}$  and  $k_y = 0.4 \text{ GeV}$  with  $\Delta_{max}$  going from 1 upto  $10^3 \text{ GeV}$ . These plots clearly justify the usage of Levin's method over the conventional Monte Carlo method. It can be seen from Fig. 1 (a) that the gluon Wigner distribution is almost constant for  $\Delta_{max} = 20 \text{ GeV}$  and beyond, where  $\Delta_{max}$  is the upper cutoff of the  $\Delta_\perp$  integration. Hence we choose the upper cutoff as  $\Delta_{max} = 20 \text{ GeV}$  for our numerical calculations, and  $m = 0.33 \text{ GeV}$ .

Now, by fixing the transverse momentum  $k_\perp = 0.4 \text{ GeV}$  we study the gluon Wigner distribution in the transverse position  $\mathbf{b}_\perp$  space for all distributions. Similarly, by fixing the impact parameter space  $b_\perp = 0.4 \text{ GeV}^{-1}$  we study the gluon Wigner distribution in the transverse momentum  $\mathbf{k}_\perp$  space. The distributions in mixed space can be studied by

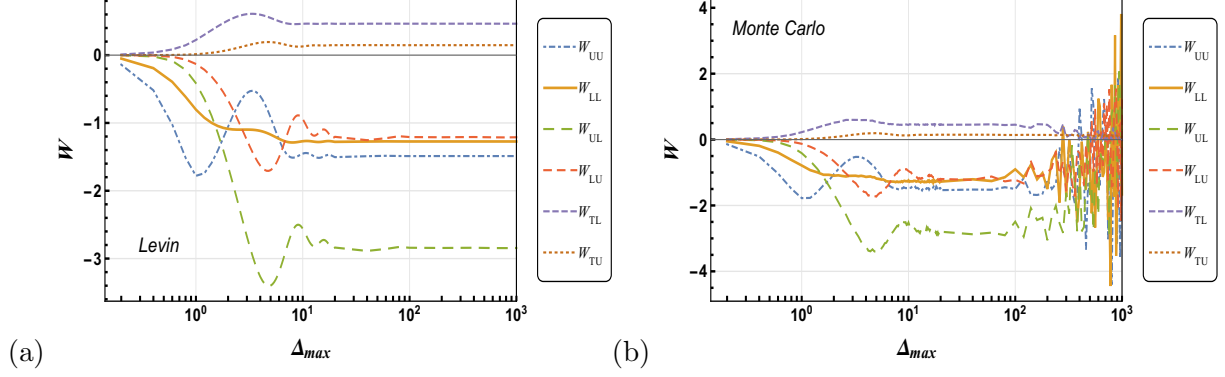


FIG. 1. Plot of six Wigner distributions vs  $\Delta_{max}$  (GeV) at a fixed value of  $b_x = 0.4 \text{ GeV}^{-1}$ ,  $b_y = 0.5 \text{ GeV}^{-1}$ ,  $k_x = 0.0 \text{ GeV}$  and  $k_y = 0.4 \text{ GeV}$  using the Levin (a) and Monte Carlo (b) integration methods.

integrating out  $b_y$  and  $k_x$  and by plotting the variables  $b_x$  and  $k_y$ . Using this numerical strategy, we first discuss the 6 independent gluon Wigner distributions. Then we discuss the remaining six distributions which are related to those through model dependent relations Eqs.(32) – (37).

Let us begin by discussing,  $W_{UU}(\mathbf{k}_\perp, \mathbf{b}_\perp)$  the Wigner distribution for an unpolarized gluon in an unpolarized dressed quark state. Figure 2 (a) shows this distribution in  $\mathbf{b}_\perp$  space with a fixed transverse momentum  $k_\perp = 0.4 \text{ GeV } \hat{e}_j$ . We observe a positive peak centered around the origin same as observed in quark Wigner distribution for same model [42]. A sharp positive peak centered around the region  $k_x = k_y = 0$  is shown in Fig 2 (b) in  $\mathbf{k}_\perp$ – space which was negative for the quark case. Thus, in the  $\mathbf{k}_\perp$ – space the quark and gluon distribution are inverted with respect to each other. This inverted behaviour is also seen in the mixed space as shown in Fig 2 (c). Figure 2 (d) shows  $W_{UL}(\mathbf{k}_\perp, \mathbf{b}_\perp)$  which is the gluon Wigner distribution for a longitudinally polarized gluon in an unpolarized target state in  $\mathbf{b}_\perp$  space with  $k_\perp = 0.4 \text{ GeV } \hat{e}_j$ . Figure. 2 (e) shows this distribution in  $\mathbf{k}_\perp$  space with fixed value of  $b_\perp = 0.4 \text{ GeV}^{-1} \hat{e}_j$ . These two plots show dipole-like structure while the mixed space plot in Fig 2(f) shows quadrupole-like behavior. Note that the behavior of  $W_{UU}$  near  $b_\perp = 0$  is determined by the relative dominance of the  $k_\perp^2$  and  $\Delta_\perp^2(1-x)^2$  terms in the numerator. As  $\Delta_{max}$  increases, the second term dominates over the first, as a result, the peak at  $b_\perp = 0$  becomes positive. As we increase  $\Delta_{max}$  beyond 20 GeV, the behavior of all Wigner distributions is independent of the cutoff.

In our model, we find that  $W_{LU}(\mathbf{k}_\perp, \mathbf{b}_\perp)$ , the unpolarized gluon in a longitudinally po-

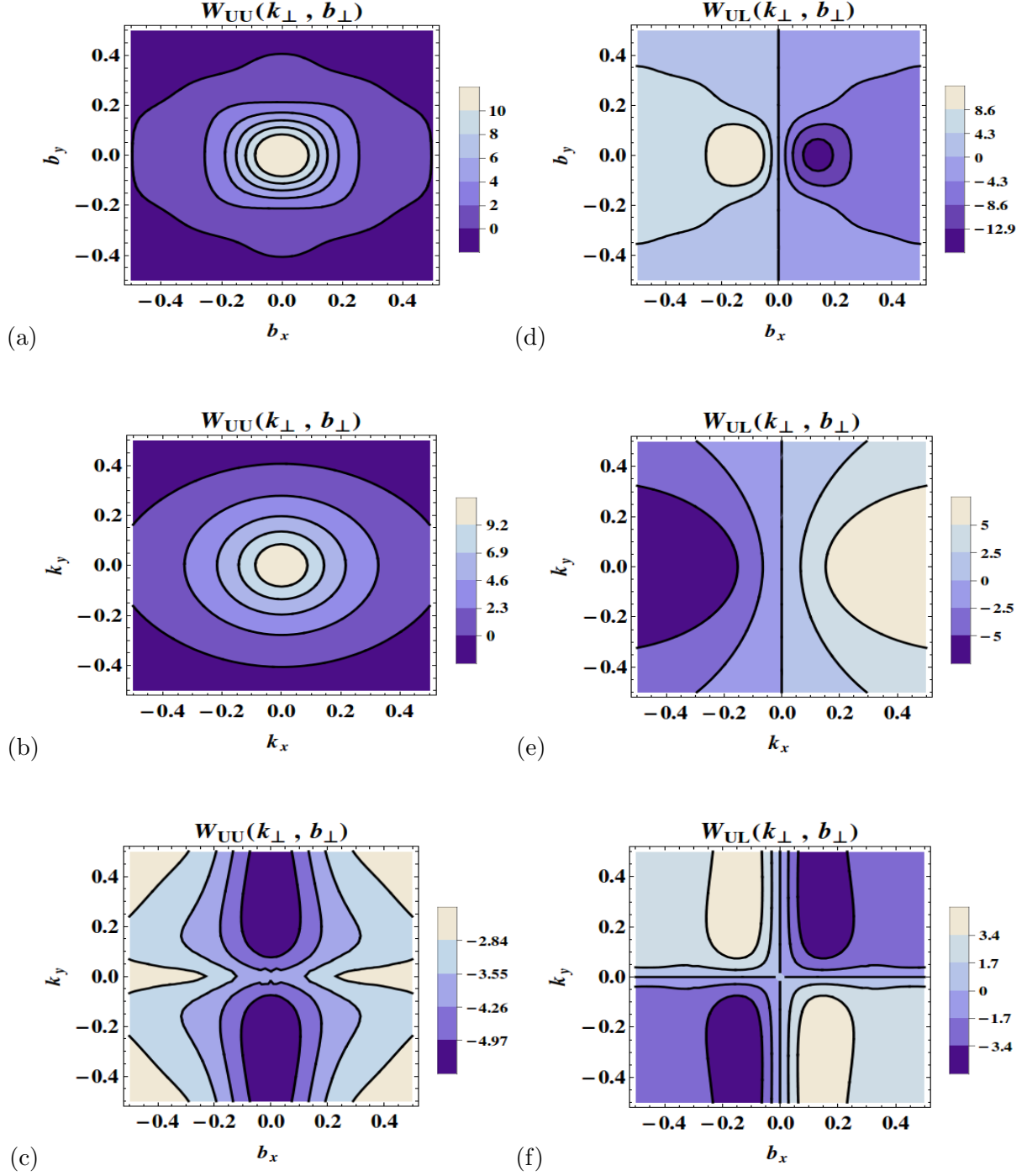


FIG. 2. Plot of gluon Wigner distributions  $W_{UU}(\mathbf{k}_\perp, \mathbf{b}_\perp)$  and  $W_{UL}(\mathbf{k}_\perp, \mathbf{b}_\perp)$  at  $\Delta_{max} = 20 \text{ GeV}$ . The first row displays the two distributions in  $\mathbf{b}_\perp$ -space with  $\mathbf{k}_\perp = 0.4 \text{ GeV} \hat{e}_y$ . The second row shows the two distributions in  $\mathbf{k}_\perp$ -space with  $\mathbf{b}_\perp = 0.4 \text{ GeV}^{-1} \hat{e}_y$ . The last row represents the two distributions in mixed space.

larized target state shows the same nature as  $W_{UL}(\mathbf{k}_\perp, \mathbf{b}_\perp)$ , the longitudinally polarized

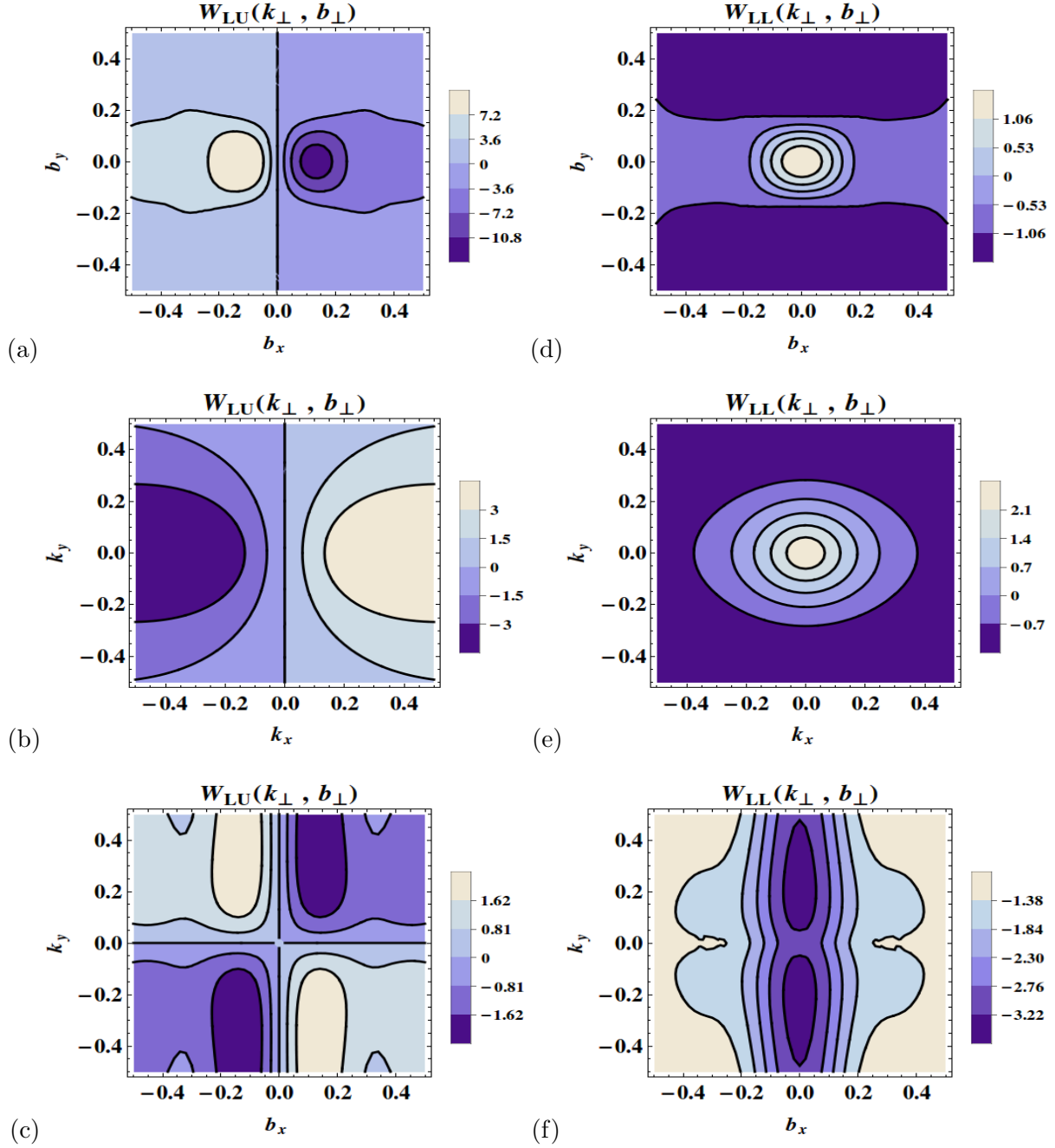


FIG. 3. Plot of Wigner distributions  $W_{LU}(\mathbf{k}_{\perp}, \mathbf{b}_{\perp})$  and  $W_{LL}(\mathbf{k}_{\perp}, \mathbf{b}_{\perp})$  at  $\Delta_{max} = 20$  GeV. The first row displays the two distributions in  $\mathbf{b}_{\perp}$ -space with  $\mathbf{k}_{\perp} = 0.4 \text{ GeV} \hat{e}_y$ . The second row shows the two distributions in  $\mathbf{k}_{\perp}$ -space with  $\mathbf{b}_{\perp} = 0.4 \text{ GeV}^{-1} \hat{e}_y$ . The last row represents the two distributions in mixed space.

gluon in an unpolarized target state as shown in Fig 3 (a) - (c) in  $\mathbf{b}_{\perp}$ ,  $\mathbf{k}_{\perp}$  and mixed space respectively. In  $\mathbf{b}_{\perp}$  and  $\mathbf{k}_{\perp}$  space, these show a dipole nature. There is no TMD limit in the

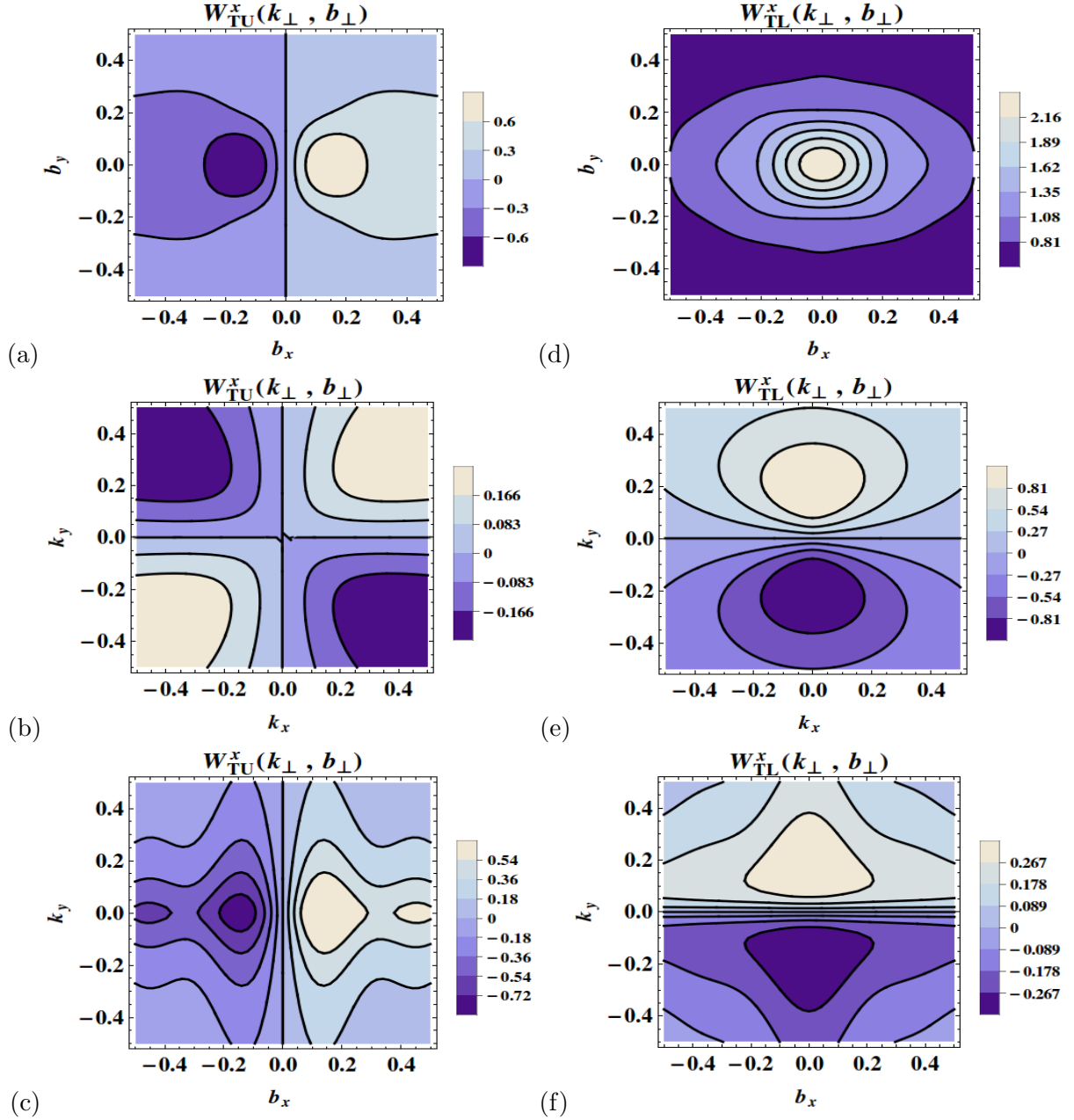


FIG. 4. Plot of Wigner distributions  $W_{TU}(\mathbf{k}_\perp, \mathbf{b}_\perp)$  and  $W_{TL}(\mathbf{k}_\perp, \mathbf{b}_\perp)$  at  $\Delta_{max} = 20 \text{ GeV}$ . The first row displays the two distributions in  $\mathbf{b}_\perp$ -space with  $\mathbf{k}_\perp = 0.4 \text{ GeV } \hat{e}_y$ . The second row shows the two distributions in  $\mathbf{k}_\perp$ -space with  $\mathbf{b}_\perp = 0.4 \text{ GeV}^{-1} \hat{e}_y$ . The last row represents the two distributions in mixed space.

Wigner distributions,  $W_{LU}(\mathbf{k}_\perp, \mathbf{b}_\perp)$  and  $W_{UL}(\mathbf{k}_\perp, \mathbf{b}_\perp)$ . These are related to the gluon orbital angular momentum (OAM) and gluon spin-orbit correlations [6]. Both the gluon OAM and the spin-orbit correlations in a dressed quark model have been calculated in [40, 47]. Similar

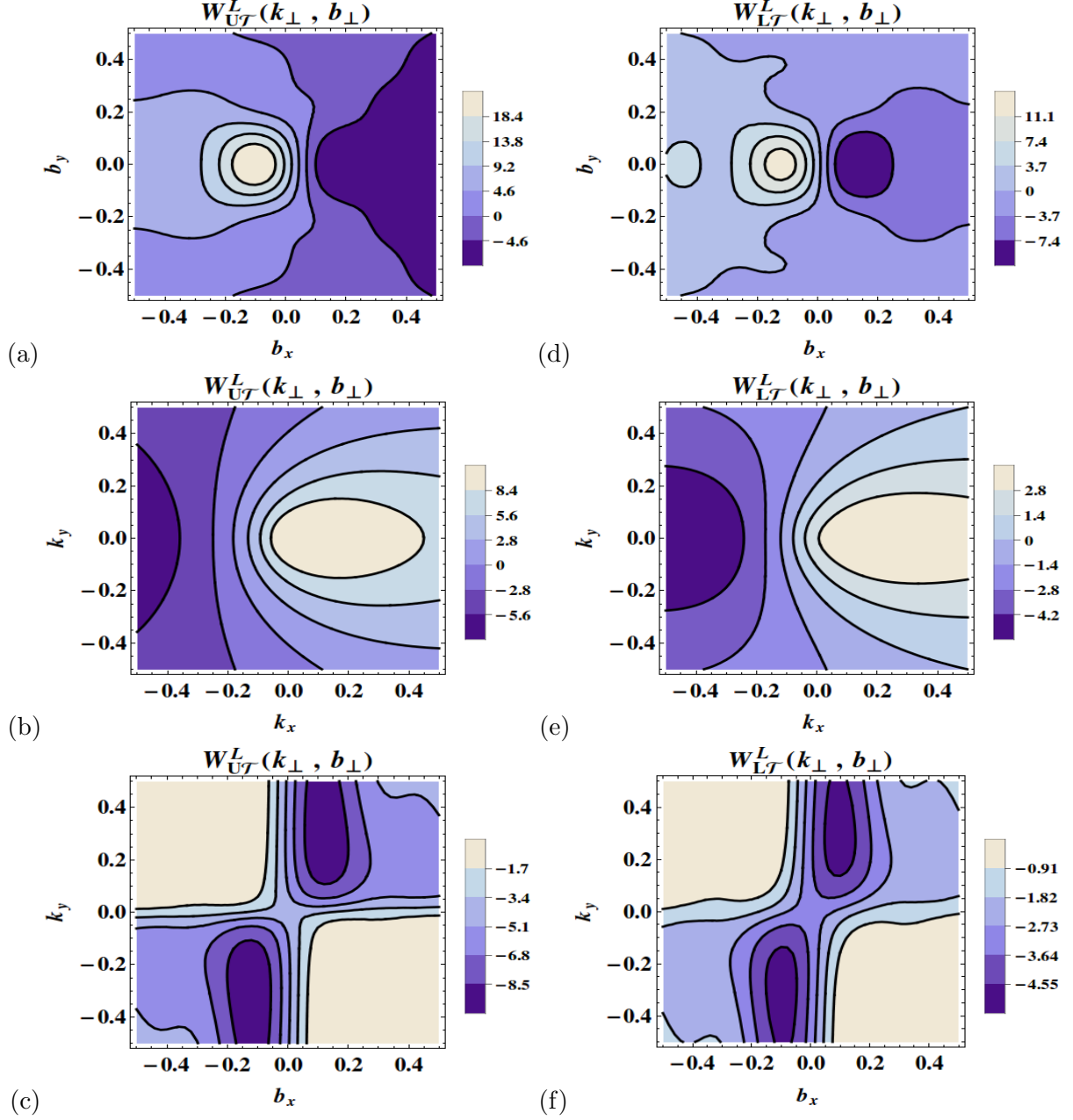


FIG. 5. Plot of Wigner distributions  $W_{U\mathcal{T}}^L(\mathbf{k}_\perp, \mathbf{b}_\perp)$  and  $W_{L\mathcal{T}}^L(\mathbf{k}_\perp, \mathbf{b}_\perp)$  at  $\Delta_{max} = 20 \text{ GeV}$ . The first row displays the two distributions in  $\mathbf{b}_\perp$ -space with  $\mathbf{k}_\perp = 0.4 \text{ GeV } \hat{e}_y$ . The second row shows the two distributions in  $\mathbf{k}_\perp$ -space with  $\mathbf{b}_\perp = 0.4 \text{ GeV}^{-1} \hat{e}_y$ . The last row represents the two distributions in mixed space.

behavior was observed in quark case for  $\mathbf{b}_\perp$ ,  $\mathbf{k}_\perp$  and mixed space respectively. In the quark case [42], the Wigner distribution for the unpolarized quark in a longitudinally polarized target state was exactly equal to a longitudinally polarized quark in an unpolarized tar-

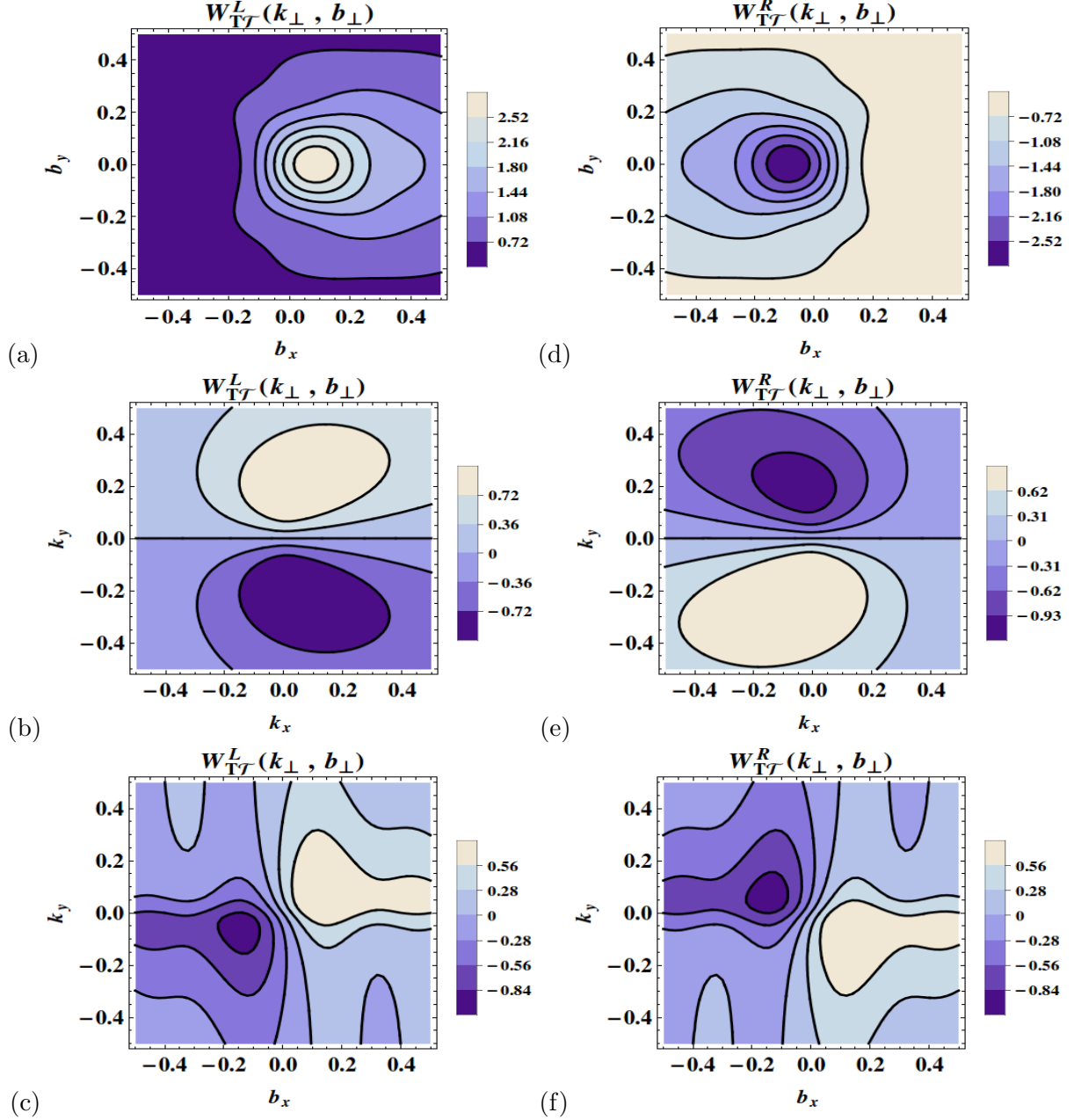


FIG. 6. Plot of Wigner distributions  $W_{TT}^L(\mathbf{k}_\perp, \mathbf{b}_\perp)$  and  $W_{TT}^R(\mathbf{k}_\perp, \mathbf{b}_\perp)$  at  $\Delta_{max} = 20$  GeV. The first row displays the two distributions in  $\mathbf{b}_\perp$ -space with  $\mathbf{k}_\perp = 0.4 \text{ GeV } \hat{e}_y$ . The second row shows the two distributions in  $\mathbf{k}_\perp$  space with  $\mathbf{b}_\perp = 0.4 \text{ GeV}^{-1} \hat{e}_y$ . The last row represents the two distributions in mixed space.

get state. But for the gluon case, we find that the two expressions for  $W_{UL}(\mathbf{k}_\perp, \mathbf{b}_\perp)$  and  $W_{LU}(\mathbf{k}_\perp, \mathbf{b}_\perp)$  [see Eqs. (25) and (26)] are not exactly equal. The difference is due to the  $x$  dependence and is washed out when performing the  $x$ -integration resulting in similar nature

of the two distributions and they differ only in their magnitude.

The Wigner distribution  $W_{LL}(\mathbf{k}_\perp, \mathbf{b}_\perp)$  shown in Fig 3 (d) describes the longitudinally polarized gluon in a longitudinally polarized target state in  $\mathbf{b}_\perp$  space. While Fig 3 (e) describes the same distribution in  $\mathbf{k}_\perp$  space. The nature of  $W_{UU}(\mathbf{k}_\perp, \mathbf{b}_\perp)$  and  $W_{LL}(\mathbf{k}_\perp, \mathbf{b}_\perp)$  in  $\mathbf{b}_\perp$  space and  $\mathbf{k}_\perp$  space are the same but differ in the magnitude which can be guessed from the analytical expression in Eqs. (24) and (27). Figure 3 (f) shows this distribution in mixed space.

Figure 4(a)-(c), shows the three dimensional plot of  $W_{TU}^x(\mathbf{k}_\perp, \mathbf{b}_\perp)$  in  $\mathbf{b}_\perp$  space,  $\mathbf{k}_\perp$  space and mixed space respectively.  $W_{TU}^x(\mathbf{k}_\perp, \mathbf{b}_\perp)$  shows dipolelike behaviour in  $\mathbf{b}_\perp$  space and mixed space whereas in  $\mathbf{k}_\perp$  space it shows quadrupole nature.  $W_{TL}^x(\mathbf{k}_\perp, \mathbf{b}_\perp)$  shows dipolelike behavior in  $\mathbf{k}_\perp$  space and mixed space. In  $\mathbf{b}_\perp$  space,  $W_{TL}^x(\mathbf{k}_\perp, \mathbf{b}_\perp)$  shows a positive peak centered at  $\mathbf{b}_\perp = 0$  owing to the cosine function.

Figure 5 (a) - (c) represents the Wigner distribution  $W_{U\mathcal{T}}^{(L)}(\mathbf{k}_\perp, \mathbf{b}_\perp)$  which corresponds to linearly polarized gluon in an unpolarized dressed quark state in  $\mathbf{b}_\perp$  space,  $\mathbf{k}_\perp$  space and mixed space respectively. This distribution is a linear combination of  $W_{UU}(\mathbf{k}_\perp, \mathbf{b}_\perp)$  and  $W_{UL}(\mathbf{k}_\perp, \mathbf{b}_\perp)$  hence one can expect the behavior of this distribution to be a slightly deformed version of  $W_{UL}(\mathbf{k}_\perp, \mathbf{b}_\perp)$ . The nature of the distribution can also be inferred from the analytical expression. However the overall nature of the distribution is similar to  $W_{UL}(\mathbf{k}_\perp, \mathbf{b}_\perp)$ . Hence in  $\mathbf{b}_\perp$  and  $\mathbf{k}_\perp$  space it shows dipolelike behavior. In mixed space, we obtain quadrupolelike nature as expected. It can be seen from Eqs. (32) and (33) that  $W_{U\mathcal{T}}^{(R)}(\mathbf{k}_\perp, \mathbf{b}_\perp)$  and  $W_{U\mathcal{T}}^{(L)}(\mathbf{k}_\perp, \mathbf{b}_\perp)$  would show similar behavior. So we do not give the plot for  $W_{U\mathcal{T}}^{(R)}(\mathbf{k}_\perp, \mathbf{b}_\perp)$  here.

The distribution  $W_{L\mathcal{T}}^{(L)}(\mathbf{k}_\perp, \mathbf{b}_\perp)$  shown in Fig 5 (d) - (f) corresponds to the linearly polarized gluon in a longitudinally polarized target state in  $\mathbf{b}_\perp$  space,  $\mathbf{k}_\perp$  space and mixed space respectively. This distribution is a linear combination of  $W_{LL}(\mathbf{k}_\perp, \mathbf{b}_\perp)$  and  $W_{LU}(\mathbf{k}_\perp, \mathbf{b}_\perp)$ . Since  $W_{UU}(\mathbf{k}_\perp, \mathbf{b}_\perp)$  is identical in nature to  $W_{LL}(\mathbf{k}_\perp, \mathbf{b}_\perp)$  and likewise  $W_{LU}(\mathbf{k}_\perp, \mathbf{b}_\perp)$  is identical to  $W_{UL}(\mathbf{k}_\perp, \mathbf{b}_\perp)$ , we find that their linear combinations are also identical in nature i.e.  $W_{U\mathcal{T}}^{(L)}(\mathbf{k}_\perp, \mathbf{b}_\perp)$  and  $W_{L\mathcal{T}}^{(L)}(\mathbf{k}_\perp, \mathbf{b}_\perp)$  shows similar behavior. The superscript notation is discussed below Eq. 15. Here we do not give the plot for  $W_{L\mathcal{T}}^{(R)}(\mathbf{k}_\perp, \mathbf{b}_\perp)$  as this distribution shows identical nature to that of  $W_{L\mathcal{T}}^{(L)}(\mathbf{k}_\perp, \mathbf{b}_\perp)$  as seen from Eqs. (34) and (35).

The Wigner distributions  $W_{T\mathcal{T}}^{(L)}(\mathbf{k}_\perp, \mathbf{b}_\perp)$  and  $W_{T\mathcal{T}}^{(R)}(\mathbf{k}_\perp, \mathbf{b}_\perp)$  corresponds to the linearly polarized gluon in a transversely polarized target state. These distributions are linear combi-

nation of  $W_{TL}^{(L)}(\mathbf{k}_\perp, \mathbf{b}_\perp)$  and  $W_{TU}^{(L)}(\mathbf{k}_\perp, \mathbf{b}_\perp)$  in this model. The effect of the linear combination on this distribution can be seen in Fig 6. The nature of the plot for  $W_{T\mathcal{T}}^{(L)}(\mathbf{k}_\perp, \mathbf{b}_\perp)$  follows closely with either  $W_{TU}^{(L)}(\mathbf{k}_\perp, \mathbf{b}_\perp)$  or  $W_{TL}^{(L)}(\mathbf{k}_\perp, \mathbf{b}_\perp)$  depending on whose overall magnitude is greater. So we see that in  $\mathbf{b}_\perp$  and  $\mathbf{k}_\perp$  space the nature is closer to  $W_{TL}^{(L)}(\mathbf{k}_\perp, \mathbf{b}_\perp)$  whereas in the mixed space it resembles the nature of  $W_{TU}^{(L)}(\mathbf{k}_\perp, \mathbf{b}_\perp)$ . For  $W_{T\mathcal{T}}^{(R)}(\mathbf{k}_\perp, \mathbf{b}_\perp)$  since the linear combination comes with a negative sign, we see that the plots for  $\mathbf{b}_\perp$  and  $\mathbf{k}_\perp$  space is inverted with respect to  $W_{T\mathcal{T}}^{(L)}(\mathbf{k}_\perp, \mathbf{b}_\perp)$ . But unlike the  $\mathbf{b}_\perp$  and  $\mathbf{k}_\perp$  space plots, the mixed space plot is not inverted since it is dominated by the contribution coming from  $W_{TU}^{(L)}(\mathbf{k}_\perp, \mathbf{b}_\perp)$ .

The GTMDs are related to various TMDs in the forward limit  $\Delta_\perp = 0$ . The GTMDs are related to the GPDs in impact parameter space upon integration over  $\mathbf{k}_\perp$ . The relation of the different GTMDs and the corresponding GPDs and TMDs are given in [24]. For operator  $\Gamma^{ij} = \delta^{ij}$ , the gluon correlator is related to the unpolarized gluon TMD  $f_1^g$  and the gluon Sivers function  $f_{1T}^{\perp g}$ . As we did not consider the gauge link at light-cone infinity, we cannot access the gluon Sivers function in this model. The GPD limit for this case gives  $H_g$  and  $E_g$ . The gluon operator with  $\Gamma^{ij} = -i \epsilon^{ij}$  is related to the gluon helicity TMD  $g_{1L}^g$  and the worm gear function  $g_{1T}^g$  (transverse helicity). The GPD limit of this operator gives  $\tilde{H}_g$  and  $\tilde{E}_g$ . In our case,  $W_{LL}(\mathbf{k}_\perp, \mathbf{b}_\perp)$  is related to the gluon helicity TMD and  $W_{TL}(\mathbf{k}_\perp, \mathbf{b}_\perp)$  is related to the worm gear function. For  $\Gamma^{ij} = \Gamma^{RR}$ , the TMD limit corresponds to four leading twist TMDs, gluon Boer-Mulders function  $h_1^{\perp g}$ , the other worm-gear function  $h_{1L}^{\perp g}$  (longitudinal transversity),  $h_{1T}^g$  which is part of gluonic transversity TMD and the gluon pretzelocity distribution,  $h_{1T}^{\perp g}$ . In our model, we cannot access the pretzelocity distribution and the worm-gear function,  $h_{1L}^{\perp g}$ , as they need the contribution of the gauge link.  $W_{U\mathcal{T}}(\mathbf{k}_\perp, \mathbf{b}_\perp)$  is related to one of the gluon Boer-Mulders functions  $h_1^{\perp g}$  [34],  $W_{T\mathcal{T}}(\mathbf{k}_\perp, \mathbf{b}_\perp)$  is related to  $h_{1T}^g$ . The GPD limit of this operator structure is related to the chiral odd GPDs.

#### IV. GLUON GTMDS AND SPIN DENSITIES RELATIONS

The analytical expressions for gluon GTMDs for the unpolarized and longitudinally polarized gluon have been discussed in [40] we will give here the expression for the new distribution that has been included in this work for the first time. It should be noted here that we use

the parameterization discussed in [48] to extract the expression of GTMD given below.

$$D_{1,1a}^{2,+} = \frac{N}{D(q_{\perp})D(q'_{\perp})} \frac{m^2}{2k_1k_2} \frac{8\left(k_1k_2 - \frac{1}{4}\Delta_1\Delta_2(1-x)^2\right)}{(1-x)x^3} \quad (38)$$

$k_1, k_2$  and  $\Delta_1, \Delta_2$  are components of  $\mathbf{k}_{\perp}$  and  $\mathbf{\Delta}_{\perp}$  respectively. As discussed before in Eq. 1, Wigner distributions are defined as a two dimensional Fourier transformation of GTMDs. Similarly, transverse densities and densities in impact parameter space are two dimensional Fourier transform of Form Factors and GPDs respectively. Analogously we integrate Wigner distributions over impact parameter space and transverse momentum space to obtain spin densities in momentum and impact parameter space respectively. Spin densities are shown in Fig. 7. For this plot, we have taken a fixed value of  $x = 0.3$ . Spin density for unpolarized gluon in an unpolarized target state, as well as longitudinally polarized gluon in a longitudinally polarized target state, are peaked at the center. Spin density for unpolarized gluon in a transversely polarized target is spread over the  $\mathbf{b}_{\perp}$  space, and the spin density for longitudinally polarized gluon in a transversely polarized target in  $\mathbf{k}_{\perp}$  space is concentrated at the center.

### A. TMD limit

TMDs can be obtained from GTMDs by taking the forward limit. In our model we set the gauge link to unity hence can access only T-even TMDs, so we display the relevant relations of gluon TMDs and GTMDs at leading twist [24].

$$f_1^g(x, \mathbf{k}_{\perp}) = \Re e[S_{1,1a}^{0+}(x, \mathbf{k}_{\perp})] \quad (39)$$

$$g_{1L}^g(x, \mathbf{k}_{\perp}) = \Re e[S_{1,1a}^{0-}(x, \mathbf{k}_{\perp})] \quad (40)$$

$$g_{1T}^g(x, \mathbf{k}_{\perp}) = \Re e[P_{1,1a}^{0-}(x, \mathbf{k}_{\perp})] \quad (41)$$

$$h_1^{\perp g}(x, \mathbf{k}_{\perp}) = 2\Re e[D_{1,1a}^{2+}(x, \mathbf{k}_{\perp})] \quad (42)$$

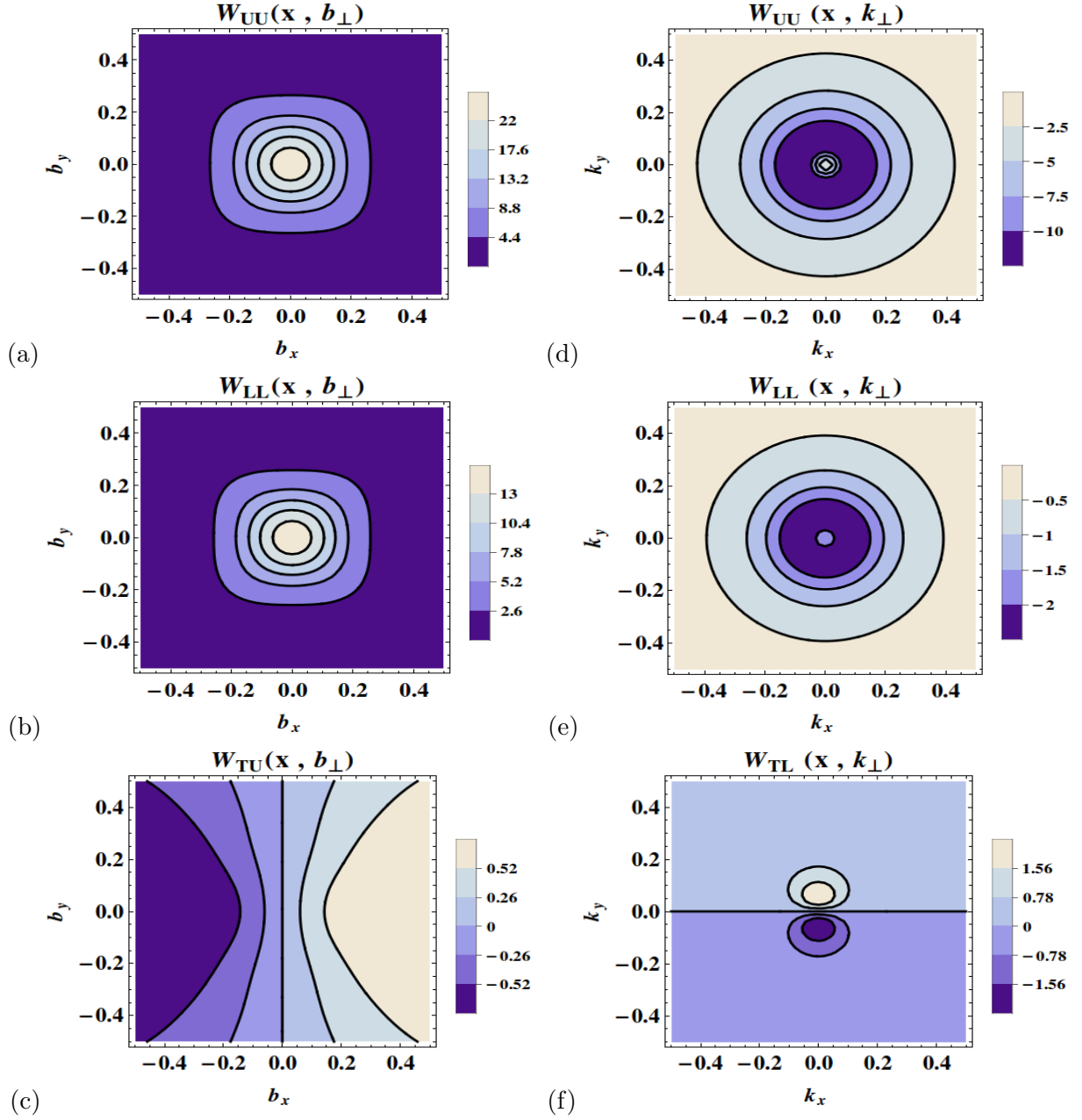


FIG. 7. Left panel shows spin densities in impact parameter space for a fixed value of  $x = 0.3$ . Right panel shows spin densities in momentum space for a fixed value of  $x = 0.3$

The corresponding analytical expressions in our model are:

$$f_1^g(x, \mathbf{k}_\perp) = \frac{2N}{x} \frac{k_\perp^2 (x^2 - 2x + 2) + m^2 x^4}{(k_\perp^2 + m^2 x^2)^2} \quad (43)$$

$$g_{1L}^g(x, \mathbf{k}_\perp) = 2N \frac{k_\perp^2 (2 - x) + m^2 x^3}{(k_\perp^2 + m^2 x^2)^2} \quad (44)$$

$$g_{1T}^g(x, \mathbf{k}_\perp) = -4Nx(1 - x) \frac{m^2}{(k_\perp^2 + m^2 x^2)^2} \quad (45)$$

$$h_1^{\perp g}(x, \mathbf{k}_\perp) = 8N \frac{(1 - x)}{x} \frac{m^2}{(k_\perp^2 + m^2 x^2)^2} \quad (46)$$

In extracting the TMDs and GPDs we have taken into account that our starting expression of the operator structure in the Wigner distribution has an overall negative sign compared to operator structure in [48]. The expressions of the TMDs in Eq. (43)-(46) match with Ref [48].

## B. GPDs in impact parameter space

Impact parameter dependent distributions (IPDs) can be obtained by integrating the Wigner distributions over the momentum space. In our model calculation we have taken the skewness parameter  $\xi$  to be zero. So the IPDs can be interpreted as the densities of gluons with longitudinal momentum fraction  $x$  in the transverse position  $\mathbf{b}_\perp$  with respect to center of momentum of the dressed quark. We integrate Wigner distribution over transverse momentum space and compare it with the parameterizations for gluon generalized correlators

in [24, 48] to obtain the IPDs.

$$\mathcal{H}^g(x, \mathbf{b}_\perp) = 2N \int [k\Delta] \frac{m^2 x^4 + (x^2 - 2x + 2) \left( \mathbf{k}_\perp^2 - \frac{1}{4} \Delta_\perp^2 (1-x)^2 \right)}{x \tilde{D}(x, \mathbf{k}_\perp, \Delta_\perp)} \quad (47)$$

$$\mathcal{E}^g(x, \mathbf{b}_\perp) = -4Nx(1-x)^2 \int [k\Delta] \frac{m^2}{\tilde{D}(x, \mathbf{k}_\perp, \Delta_\perp)} \quad (48)$$

$$\tilde{\mathcal{H}}^g(x, \mathbf{b}_\perp) = 2N \int [k\Delta] \frac{m^2 x^3 + (2-x) \left( \mathbf{k}_\perp^2 - \frac{1}{4} \Delta_\perp^2 (1-x)^2 \right)}{\tilde{D}(x, \mathbf{k}_\perp, \Delta_\perp)} \quad (49)$$

$$\mathcal{H}_T^g(x, \mathbf{b}_\perp) = -4Nx(1-x) \int [k\Delta] \frac{m^2}{\tilde{D}(x, \mathbf{k}_\perp, \Delta_\perp)} \quad (50)$$

$$\mathcal{E}_T^g(x, \mathbf{b}_\perp) = -16N \frac{(1-x)}{x} \int [k\Delta] \frac{\frac{m^2}{\Delta_1 \Delta_2} (k_1 k_2 - \frac{1}{4} (1-x)^2 \Delta_1 \Delta_2)}{\tilde{D}(x, \mathbf{k}_\perp, \Delta_\perp)} \quad (51)$$

$$\tilde{\mathcal{H}}_T^g(x, \mathbf{b}_\perp) = 0 \quad (52)$$

where

$$\int [k\Delta] = \int d^2 \mathbf{k}_\perp \int \frac{d^2 \Delta_\perp \cos(\Delta_\perp \mathbf{b}_\perp)}{2(2\pi)^2} \quad (53)$$

$$\tilde{D}(x, \mathbf{k}_\perp, \Delta_\perp) = \left( \left( \mathbf{k}_\perp + \frac{\Delta_\perp (1-x)}{2} \right)^2 + m^2 x^2 \right) \left( \left( \mathbf{k}_\perp - \frac{\Delta_\perp (1-x)}{2} \right)^2 + m^2 x^2 \right) \quad (54)$$

Thus, in our model  $\tilde{\mathcal{E}}^g$  and  $\tilde{\mathcal{E}}_T^g$  do not contribute since we have chosen  $\xi = 0$ . The relations we obtain in Eq. (47) – (52) are in agreement with the GPDs obtained in [48].

## V. GLUON ORBITAL ANGULAR MOMENTUM AT SMALL- $x$

The canonical OAM distribution for the gluon is obtained from the GTMD [6, 37],

$$l_g(x) = - \int d^2 \mathbf{k}_\perp \frac{\mathbf{k}_\perp^2}{m^2} S_{1,1b}^{0+}(x, \mathbf{k}_\perp) \quad (55)$$

Gluon helicity is obtained from the other GTMD,

$$\Delta G(x) = \frac{1}{2} \int d^2 \mathbf{k}_\perp S_{1,1b}^{0-}(x, \mathbf{k}_\perp) \quad (56)$$

By comparing the operator structures in the above two cases for small  $x$ , the following relation between the gluon OAM and gluon helicity was pointed out by Hatta *et.al.* [25]

(note that the  $l_g$  used in this reference has a difference in a factor of 2 compared to ours, as seen from Eq. (32) in Ref [25]):

$$l_g(x) \approx -\Delta G(x) \quad (57)$$

It would interesting to see if this relation holds for a dressed quark target. The gluon GTMDs in the dressed quark model was evaluated in Ref. [40] at the leading twist. The gluon canonical orbital angular momentum  $l_g(x)$  was also calculated using these GTMDs. Because of a negative sign in the operator structure of our starting expression of the Wigner distribution as compared to [49], we need an extra negative sign on the right-hand side of Eq. (56), in order to compare with [49] in the massless limit. The analytic expressions for  $l_g(x)$  and  $\Delta G(x)$  are given by

$$l_g(x) = -N(1-x)(2-x) [I - \pi] \quad (58)$$

$$\Delta G(x) = N [(x-2)I + 2\pi(1-x)] \quad (59)$$

where

$$I = \pi \log \left( \frac{Q^2 + m^2 x^2}{\mu^2 + m^2 x^2} \right) \quad (60)$$

Here  $Q$  and  $\mu$  are the upper and lower cutoff on  $\mathbf{k}_\perp$ . The expressions for  $l_g(x)$  and  $\Delta G(x)$

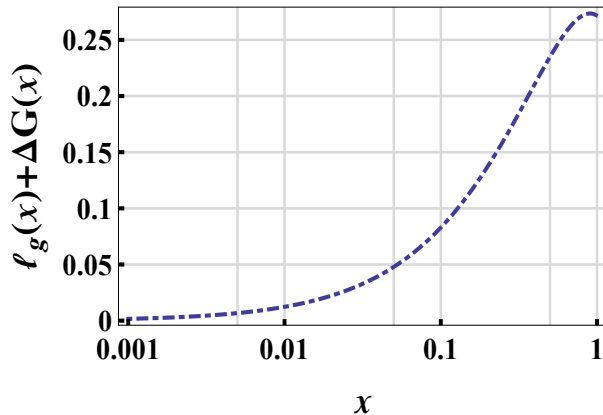


FIG. 8. Plot of  $l_g(x) + \Delta G(x)$  vs  $x$ . Here we choose,  $Q = 10$  GeV,  $\mu = 0.0$  GeV,  $m = 0.33$  GeV and  $N = \frac{1}{2(2\pi)^2}$

in Eqs. (56) and (59) is same as in [49] in the case of massless limit. Figure 8 shows that for small- $x$  the relation  $l_g(x) \approx -\Delta G(x)$  holds for a dressed quark target.

## VI. CONCLUSION

In this work, we have investigated the gluon Wigner distributions for unpolarized, longitudinally polarized and transversely polarized target state, taking into account all possible polarization combinations of the gluon at leading twist. Instead of a proton target, we took a quark state dressed with a gluon, which acted as a perturbative model of a composite spin-1/2 state, and made it possible to investigate the gluon Wigner distributions, unlike most phenomenological models without a gluonic degree of freedom. We improved the numerical convergence compared to an earlier study with respect to the upper limit on  $\Delta_{\perp}(\Delta_{max})$ , as a result, the Wigner distributions presented here are independent of  $\Delta_{max}$ . We study the leading twist gluon Wigner distributions, out of which 6 are independent Wigner distributions, and the remaining are linear combinations of those. All the distributions are expressed as overlaps of light-front wave functions and are calculated using an analytic form of the wave functions in light-cone gauge, they are presented in the transverse position, transverse momentum and mixed space. We have chosen light-cone gauge and have taken the gauge link to be unity. We obtained the GTMDs and calculated the spin densities in transverse momentum and position space. We have shown that at small- $x$ , gluon OAM is related to the gluon helicity in this model. Further work in this line would be to investigate the effect of the gauge link on the Wigner distributions and TMDs.

- 
- [1] S. Meissner, A. Metz and M. Schlegel, *JHEP* **0908**, 056 (2009).
  - [2] E. P. Wigner, *Phys. Rev.* **40**, 749 (1932).
  - [3] X. D. Ji, *Phys. Rev. Lett.* **91**, 062001 (2003).
  - [4] A. V. Belitsky, X. D. Ji and F. Yuan, *Phys. Rev. D* **69**, 074014 (2004).
  - [5] M. Burkardt and B. Pasquini, *Eur. Phys. J. A* **52**, 161 (2016).
  - [6] C. Lorcé and B. Pasquini, *Phys. Rev. D* **84**, 014015 (2011).
  - [7] P. J. Mulders and J. Rodrigues, *Phys. Rev. D* **63**, 094021 (2001).
  - [8] X. D. Ji, J. P. Ma and F. Yuan, *JHEP* **0507**, 020 (2005).
  - [9] K. Goeke, A. Metz and M. Schlegel, *Phys. Lett. B* **618**, 90 (2005).
  - [10] K. Goeke, M. V. Polyakov and M. Vanderhaeghen, *Prog. Part. Nucl. Phys.* **47**, 401 (2001).
  - [11] M. Diehl, *Eur. Phys. J. C* **25**, 223 (2002); Erratum: [*Eur. Phys. J. C* **31**, 277 (2003)].

- [12] M. Diehl, Phys. Repts. **388**, 41 (2003).
- [13] X. Ji, Ann. Rev. Nucl. Part. Sci. **54**, 413 (2004).
- [14] A. V. Belitsky and A. V. Radyushkin, Phys. Rept. **418**, 1 (2005).
- [15] S. Boffi and B. Pasquini, Riv. Nuovo Cim. **30**, 387 (2007).
- [16] X. D. Ji, Phys. Rev. Lett. **78**, 610 (1997).
- [17] T. Liu and B. Q. Ma, Phys. Rev. D **91**, 034019 (2015).
- [18] D. Chakrabarti, T. Maji, C. Mondal and A. Mukherjee, Eur. Phys. J. C **76**, 409 (2016).
- [19] D. Chakrabarti, T. Maji, C. Mondal and A. Mukherjee, Phys. Rev. D **95**, 074028 (2017).
- [20] Y. V. Kovchegov and M. D. Sievert, Nucl. Phys. B **903**, 164 (2016).
- [21] S. Bhattacharya, A. Metz and J. Zhou, Phys. Lett. B **771**, 396 (2017).
- [22] A. D. Martin, M. G. Ryskin and T. Teubner, Phys. Rev. D **62**, 014022 (2000).
- [23] V. A. Khoze, A. D. Martin and M. G. Ryskin, Eur. Phys. J. C **14**, 525 (2000).
- [24] C. Lorcé and B. Pasquini, JHEP **1309**, 138 (2013).
- [25] Y. Hatta, Y. Nakagawa, F. Yuan and Y. Zhao, Phys. Rev. D **95**, 114032 (2017).
- [26] Y. Hatta, B. W. Xiao and F. Yuan, Phys. Rev. Lett. **116**, 202301 (2016).
- [27] T. Altinoluk, N. Armesto, G. Beuf and A. H. Rezaeian, Phys. Lett. B **758**, 373 (2016).
- [28] J. Zhou, Phys. Rev. D **94**, 114017 (2016).
- [29] Y. Hatta, B. W. Xiao and F. Yuan, Phys. Rev. D **95**, 114026 (2017).
- [30] Y. Hagiwara, Y. Hatta and T. Ueda, Phys. Rev. D **94**, 094036 (2016).
- [31] Y. Hagiwara, Y. Hatta, R. Pasechnik, M. Tasevsky and O. Teryaev, Phys. Rev. D **96**, 034009 (2017).
- [32] C. J. Bomhof, P. J. Mulders and F. Pijlman, Eur. Phys. J. C **47**, 147 (2006).
- [33] C. J. Bomhof and P. J. Mulders, Nucl. Phys. B **795**, 409 (2008).
- [34] M. G. A. Buffing, A. Mukherjee and P. J. Mulders, Phys. Rev. D **88**, 054027 (2013).
- [35] P. Hagler, A. Mukherjee and A. Schafer, Phys. Lett. B **582**, 55 (2004).
- [36] C. Lorcé, B. Pasquini, X. Xiong and F. Yuan, Phys. Rev. D **85**, 114006 (2012)
- [37] Y. Hatta, Phys. Lett. B **708**, 186 (2012).
- [38] M. Burkardt, Phys. Rev. D **88**, 014014 (2013).
- [39] X. Ji, F. Yuan and Y. Zhao, Phys. Rev. Lett. **118**, 192004 (2017).
- [40] A. Mukherjee, S. Nair and V. K. Ojha, Phys. Rev. D **91**, 054018 (2015).
- [41] A. Mukherjee, S. Nair and V. K. Ojha, Phys. Rev. D **90**, 014024 (2014).

- [42] J. More, A. Mukherjee and S. Nair, Phys. Rev. D **95**, 074039 (2017).
- [43] A. Harindranath, R. Kundu and W. M. Zhang, Phys. Rev. D **59**, 094012 (1999); Phys. Rev. D **59**, 094013 (1999).
- [44] D. Levin, Math. Comp. **38**, 531 (1982).
- [45] D. Levin, J. Comput. Appl. Maths **67**, 95 (1996).
- [46] D. Levin, J. Comput. App. Maths **78**, 131 (1997).
- [47] K. Kanazawa, C. Lorcé, A. Metz, B. Pasquini and M. Schlegel, Phys. Rev. D **90**, 014028 (2014).
- [48] S. Meissner, A. Metz and K. Goeke, Phys. Rev. D **76**, 034002 (2007).
- [49] A. Harindranath and R. Kundu, Phys. Rev. D **59**, 116013 (1999).